

# Performance of Close Anode Cathodic Protection System Applied to a Plane Metallic Grid

E. M. Saad El-Deen Noamy, A. S. Abd El-Ghany, S. M. Desouky, A. Gomaa

**Abstract**— In CP technique the negative shift in cathode potential determines the degree of protection against corrosion. This shift occurs by two mechanisms: the first is depression of cathode potential relative to electrolyte (Remote Anode Systems). The second is elevation of electrolyte potential in the vicinity of cathode relative to electrolyte (Close Anode Systems). These systems are considerably sensitive to anode position because of sharp changes in electrolyte potential with variation of anode location (proximity effect). Our work is to investigate the performance of CP system under conditions of variable anode position, applied to mild steel grid simulating steel reinforced concrete.

**Index Terms**— Cathodic protection; Potential parameters; Polarization; Mild steel; Steel reinforced concrete.

## I. INTRODUCTION

Cathodic Protection (CP) technique has acquired wide recognition as a powerful tool for mitigation of corrosion damage, particularly in steel reinforced concrete (SRC) structures. When the structure are exposed to marine atmosphere, in such cases chloride ions penetrates the concrete cover and damage the passive oxide layer naturally formed on reinforcing steel.

CP system consists essentially of [1]:

- i. Cathode, which is the metal to be protected,
- ii. Anode, which is the metal put intentionally to corrode instead of cathode and
- iii. DC current source

Current flows from cathode to anode electronically through a conductor cable, and the circuit is completed from anode to cathode ionically through surrounding media (electrolyte).

There are two types of CP systems [2]:

- a. Sacrificial Anode System (SAS), in which the anode has a lower natural potential than the cathode, the required DC is generated by battery action between the two poles (anode & cathode), Figure (1).
- b. Impressed Current System (ICS), in which required DC is supplied by external source, Figure (2).

Both types are applicable to SRC protection.

Corrosion byproducts precipitated on anode surface may restrict system performance due to its low electric conductivity. In extreme cases, such products may cause cracks in concrete layer above anodes, which in turn

promotes additional corrosion hazard. To avoid such unfavorable protection side effects, it is a common practice to use inert anodes with impressed current systems (Titanium alloys or Platinum coated anodes) where no deposits are formed on anode surface [3]. With SAS, the common practice is to use porous Zinc anodes with special chemical activators to generate soluble corrosion byproducts [4].

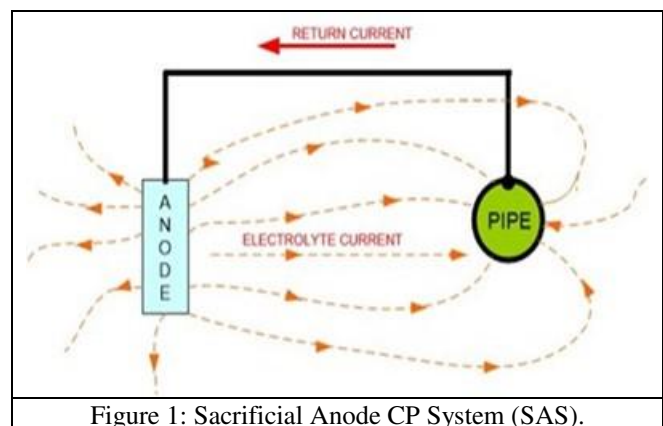


Figure 1: Sacrificial Anode CP System (SAS).

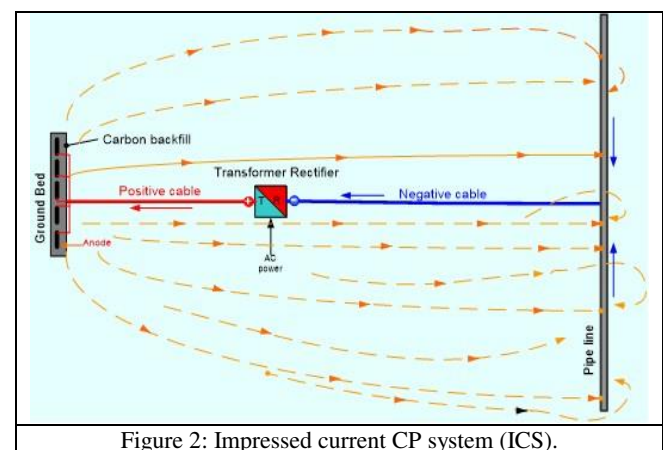


Figure 2: Impressed current CP system (ICS).

Due to space limitations, cathodic protection for SRC structures is essentially achieved by using “Close Anode” technique, where cathode potential shift and consequently, degree of protection is determined mainly by distance from anode. Because of this fact, structures protected by “Close Anodes” could have wide variation in protection level over its exposed surface [5].

Close Anodes may induce the so called “Shading Phenomenon”, where cathode surface facing the anode absorbs most of incoming electric current flux leaving back surfaces with little or no protection. Such phenomenon was observed in laboratory experimental works on a steel plate[6], when the plate was protected by “Close Anodes” located at

**Dr.E. M. Saad El-Deen Noamy**, Egyptian Petroleum Research Institute, Cairo, (Egypt).

**Prof. Dr.Saad Desouky**, Egyptian Petroleum Research Institute, Cairo, (Egypt).

**Prof. Dr. Ahmed Shawky Abd El-Ghany**, Faculty of Engineering, Ain Shams University, Cairo, (Egypt).

**Dr. Ali Gomaa**, Egyptian Petroleum Research Institute, Cairo, (Egypt).

one side, the back side of the plate revealed much less protection.

## II. EXPERIMENTAL

Experiments were carried out on a specially constructed arrangement consisting of the following:

1. Fiber glass basin 900×900×300 mm containing electrolyte (NaCl solution, 3.5%wt concentration) 250 mm depth. The solution is almost the same as sea water salinity [7].
2. Mild steel expanded metal grid 600×600×5 mm simulating reinforcing steel bars (Rebar) in concrete, Figure (3). The grid was supported 120 mm above bottom of basin on four Teflon posts. Grid potential and current drain were measured through four mild steel  $\phi 3$  mm conductors welded one at each corner and one conductor at center point of the grid [8].
3. Four cubic zinc anodes 20×20×20 mm, each with a steel tail of  $\phi 3$  mm and 315 mm length for connection to the grid, Figure (4).
4. A reference zinc electrode incased in a PVC tube in a way to keep constant distance of 5 mm between zinc tip and grid surface during measurement [9].
5. A highly precise digital multimeter was used to measure grid/electrolyte potential difference, voltage and current of the system.

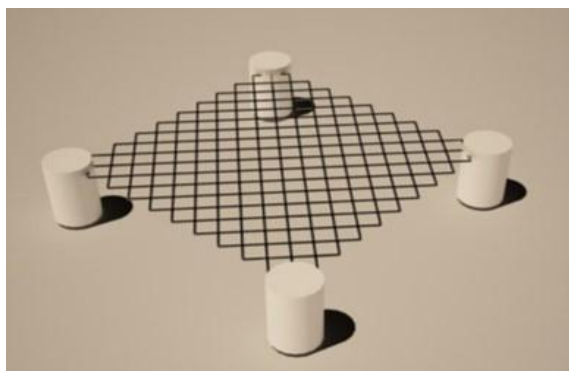


Figure 3: Grid and Teflon support.



Figure 4: Anodes and tails.

## III. WORK PROCEDURE

System performance was investigated for three different anodes configurations:

1. Grouped anodes with single drain point at the center of the grid (configuration i).
2. Grouped anodes with four drain points at grid corners (configuration ii).
3. Distributed anodes with individual drain at each corner (configuration iii).

For each anodes configuration, three locations were considered:

1. Anodes located in the same level of the grid (mode a)
2. Anodes located 50 mm above the grid (mode b)
3. Anode located 50 mm below the grid (mode c)

Current flow paths in the three locations and the electric current circuit are represented diagrammatically in Figure (5& 6).

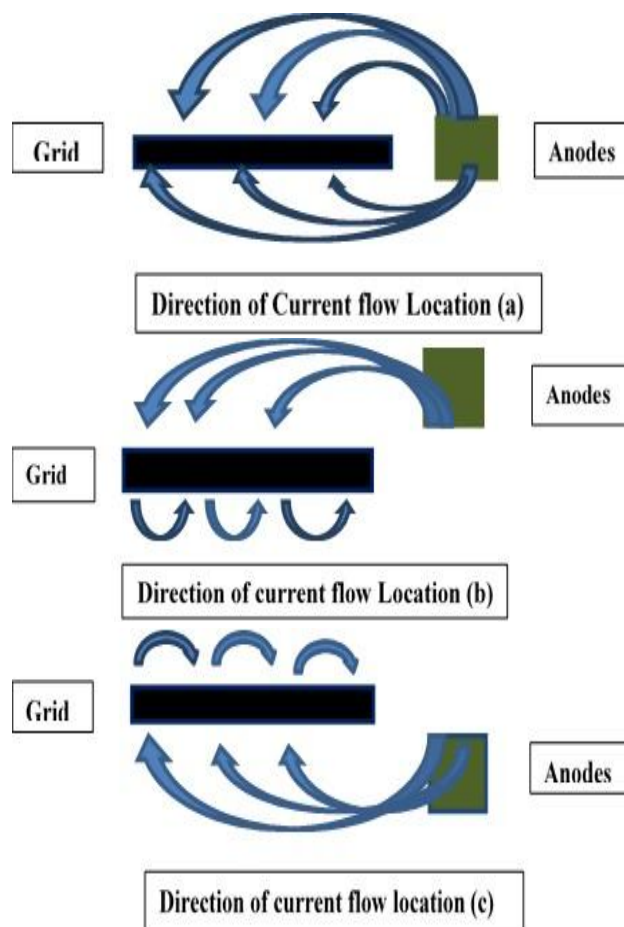


Figure (5): Schematic diagram of current flow direction

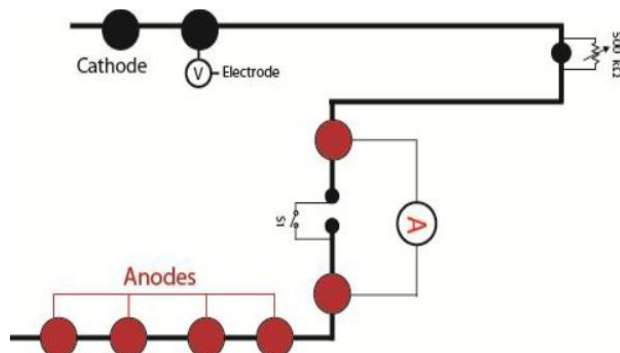


Figure (6): Schematic diagram of the electric current circuit

Investigated anodes configurations and locations are illustrated in Figures (7 to 12).

Grid potentials were measured by placing the reference electrode tip on the grid at the corners and center point for the

three locations of each configuration.

Potentials were recorded at each point after sufficient stabilization time. The average of three readings with one-day interval for each measuring point was considered [10].

In this manner, it was possible to assess the proximity effect by measuring potential at different distances from anodes, as well as the effect of electric flux shading by the grid when the anodes location level was changed.

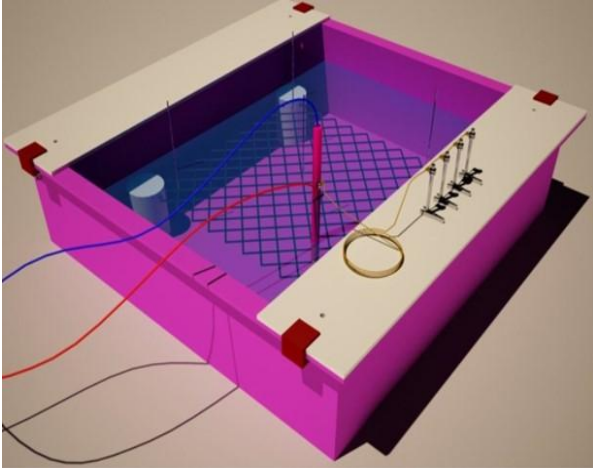


Figure 7: An actual image of configuration i.

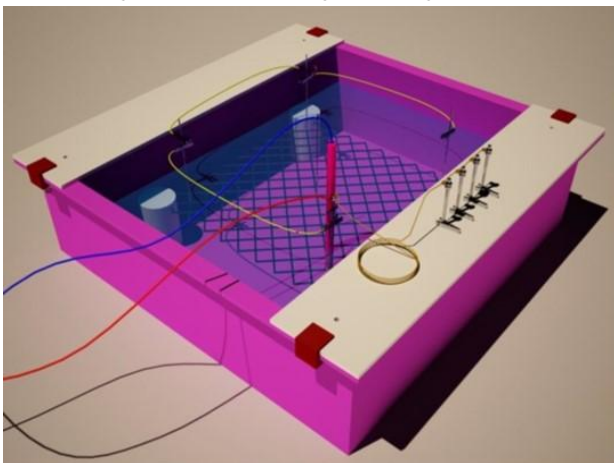


Figure 8: An actual image of configuration ii.

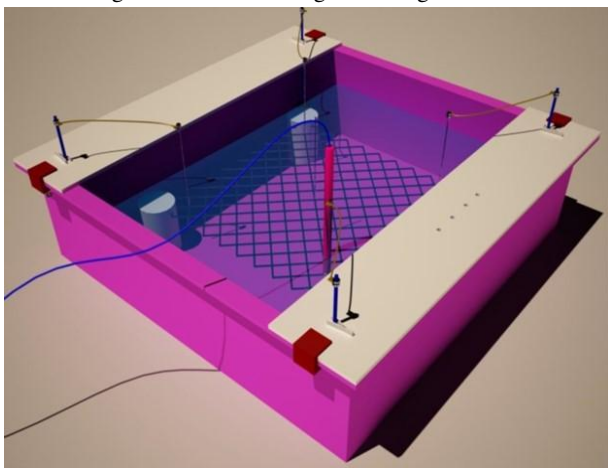


Figure 9: An actual image of configuration iii.

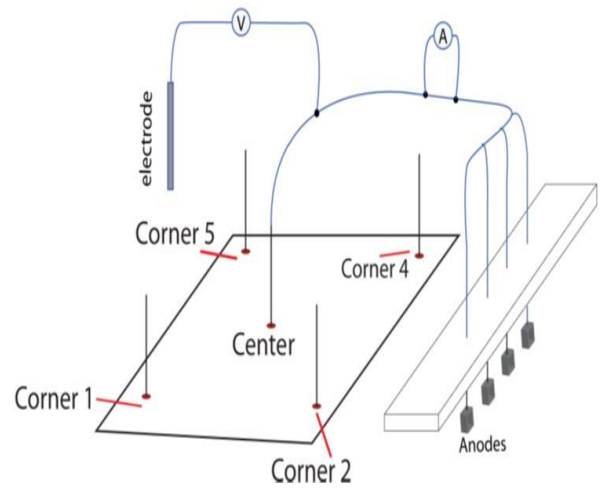


Figure 10: Schematic diagram configuration i

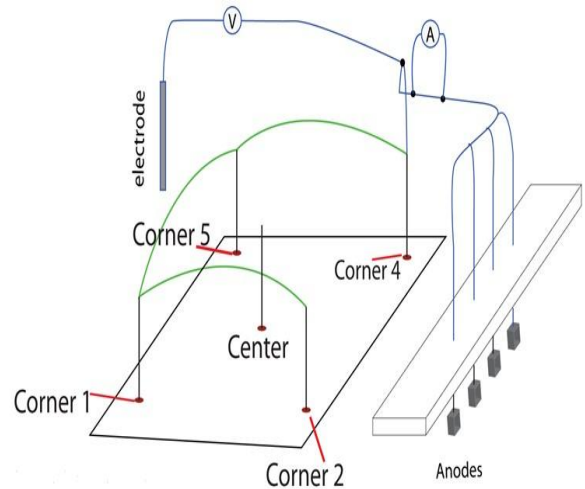


Figure 11: Schematic diagram configuration ii

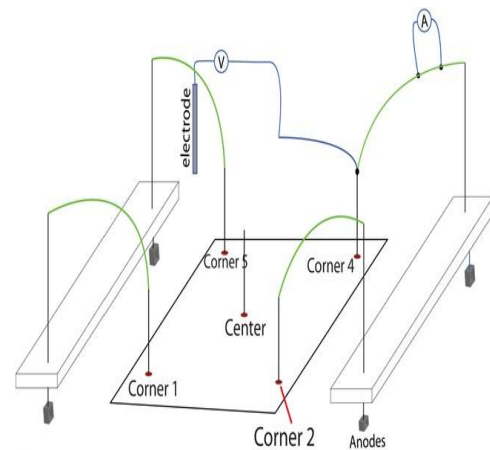


Figure 12: Schematic diagram configuration iii

#### IV. RESULTS AND DISCUSSION

Experimental data obtained from this work, are presented in Table (1 to 3) and Figures (13 to 30). Examination of these data reveals the following results for the studied system configurations:

##### A. Distributed Anodes System Configuration (iii)

- The configuration of this case is shown in Figures (9 & 12). In general, this configuration provided the best protection level for the steel grid as

illustrated in Table (1) and Figures (25 to 30).

- Grid potential at center point was slightly more positive than at corners; which reflects mild “Proximity” effect phenomenon.
- Anodes location (a) arrangement (anode at the same level of the grid) provided considerably better potential than the two other locations. This is an indicator for shading phenomenon mentioned before.
- Current consumption in this case was much more than the other two configurations. Obviously, this can be attributed to the lower gross resistance of separated anodes than that of grouped one.

**B. Grouped Anodes Multi Drain Points Configuration (ii)**

- The configuration of this case is shown in Figures (8&11). This configuration provided less protection than configuration (iii), but consumed the lowest current among the three studied configurations.
- Proximity effect was clear in all considered locations (a, b & c). Grid potential increased with distance from anodes, Table (2) and Figures (19 to 24).
- Protection level with anodes above grid level, location (b) was better than anodes below grid, location (c). This is mostly attributed to shading effect.

**C. Grouped Anodes single Drain Point Configuration (i)**

- The configuration of this case is shown in Figures (7& 10). This system arrangement exhibited the lowest performance among the studied configurations, Table (3) and Figures (13 to 18)
- Both proximity and shading effects were observed in this case.
- Low current consumption (almost same at configuration (ii)) was due to anode resistance.

**Table 1: Configuration iii**

Mode	Position	$\Delta V$ (ON) mV	$\Delta V$ (OFF) mV	$\Delta E$ mV	Current mA	Grid Resistance $\Omega$
a	corner 1	110	115	5.0	0.513	10.526
	corner 2	105	108	3.0		
	center	123	129	6.0		
	corner 4	104	110	6.0		
	corner 5	116	123	7.0		
b	corner 1	118.0	122.5	4.5	0.516	12.015
	corner 2	114.5	122.5	8.0		
	center	127.0	134.0	7.0		
	corner 4	112.0	117.5	5.5		
	corner 5	124.5	130.5	6.0		
c	corner 1	119.5	127	7.5	0.520	14.23
	corner 2	120	129	9.0		
	center	134	140.5	6.5		
	corner 4	114	118.5	4.5		
	corner 5	124	133.5	9.5		

**Table 2: Configuration ii**

Mode	Position	$\Delta V$ (ON) mV	$\Delta V$ (OFF) mV	$\Delta E$ mV	Current mA	Grid Resistance $\Omega$
a	corner 1	153	159	6.0	0.193	42.48
	corner 2	143	151	8.0		
	center	146	156	10.0		
	corner 4	142	154	12.0		
	corner 5	151	156	5.0		
b	corner 1	159.0	163.5	4.5	0.172	34.3
	corner 2	156.5	162.0	5.5		
	center	158.0	165.5	7.5		
	corner 4	155.0	161.5	6.5		
	corner 5	163.5	169.0	5.5		
c	corner 1	169	173.5	4.5	0.182	35.71
	corner 2	155.5	162	6.5		
	center	162	171	9.0		
	corner 4	156	164	8.0		
	corner 5	167	171.5	4.5		

**Table 3: Configuration i**

Mode	Position	$\Delta V$ (ON) mV	$\Delta V$ (OFF) mV	$\Delta E$ mV	Current mA	Grid Resistance $\Omega$
a	corner 1	176	181	5.0	0.192	28.125
	corner 2	158	166	8.0		
	center	168	175	7.0		
	corner 4	162	168	6.0		
	corner 5	177	181	4.0		
b	corner 1	173.5	180.0	6.5	0.193	32.64
	corner 2	162.0	167.5	5.5		
	center	170.0	176.5	6.5		
	corner 4	165.5	171.5	6.0		
	corner 5	172.0	179.0	7.0		
c	corner 1	174	179.5	5.5	0.189	32.74
	corner 2	164	169.5	5.5		
	center	173	178.5	5.5		
	corner 4	168	172.5	4.5		
	corner 5	178.5	184.5	6.0		

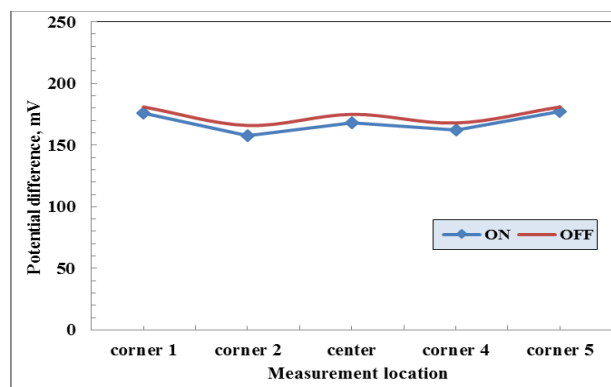


Figure 13: Average potential [ON & OFF] for configuration (i) location (a)

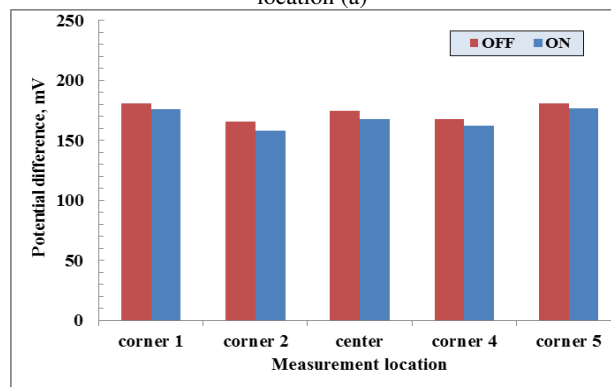


Figure 14: Polarization chart for configuration (i) location (a)

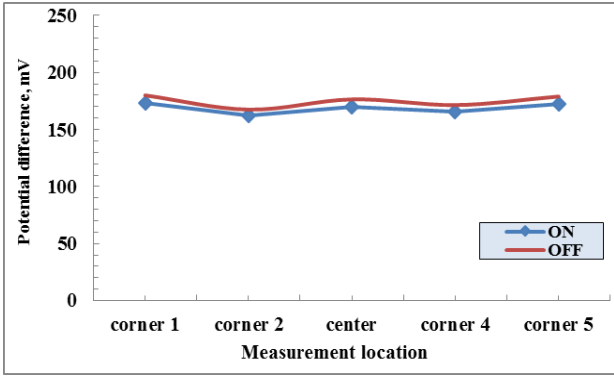


Figure 15: Average potential [ON & OFF] for configuration (i) location (b)

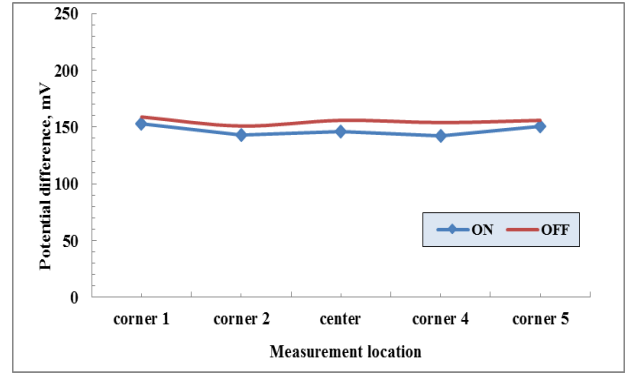


Figure 19: Average potential [ON & OFF] for configuration (ii) location (a)

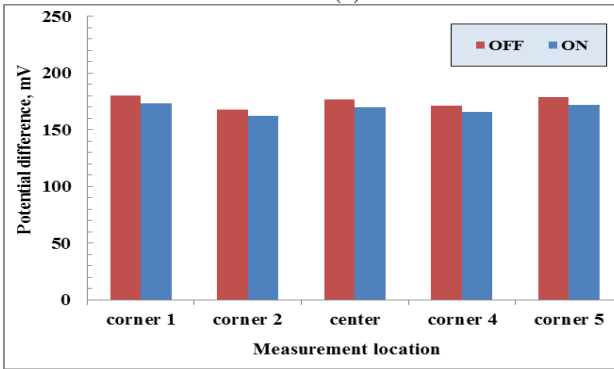


Figure 16: Polarization chart for configuration (i) location (b)

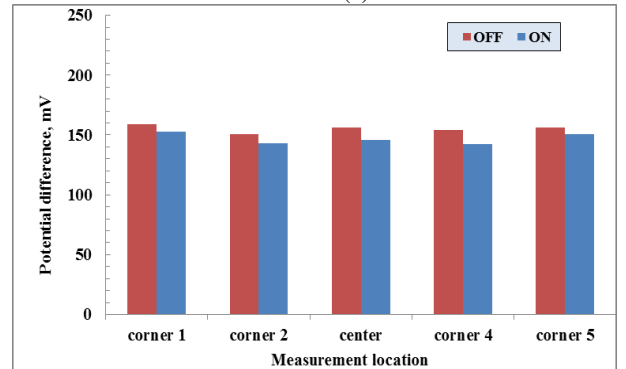


Figure 20: Polarization chart for configuration (ii) location (a)

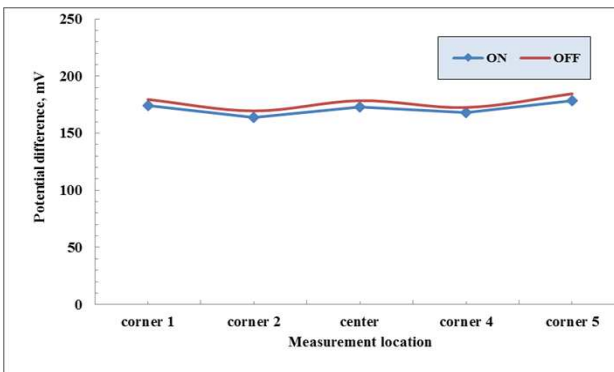


Figure 17: Average potential [ON & OFF] for configuration (i) location (c)

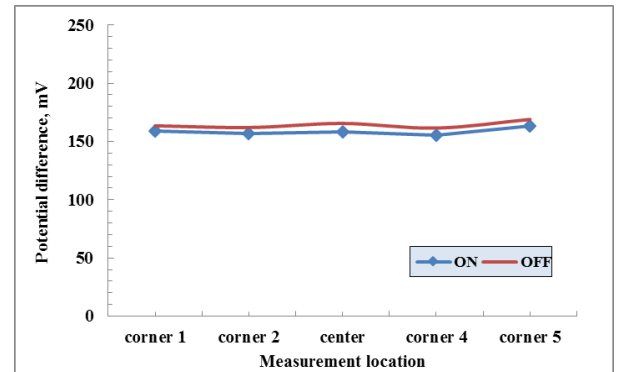


Figure 21: Average potential [ON & OFF] for configuration (ii) location (b)

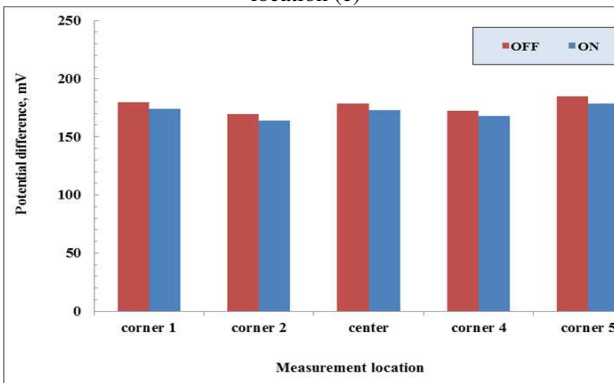


Figure 18: Polarization chart for configuration (i) location (c)

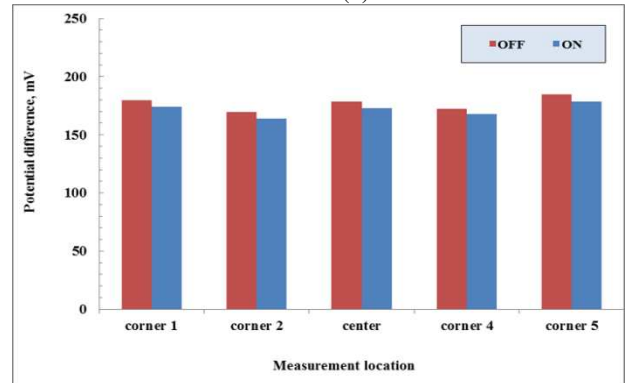


Figure 22: Polarization chart for configuration (ii) location (b)

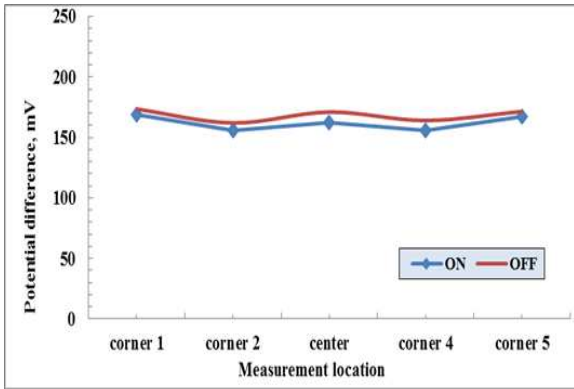


Figure 23: Average potential [ON& OFF] for configuration (ii) location (c)

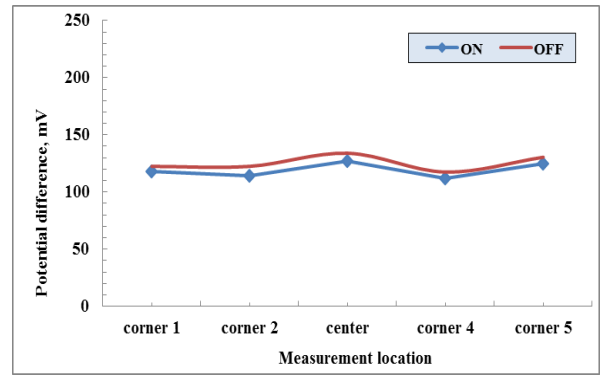


Figure 27: Average potential [ON& OFF] for configuration (iii) location (b)

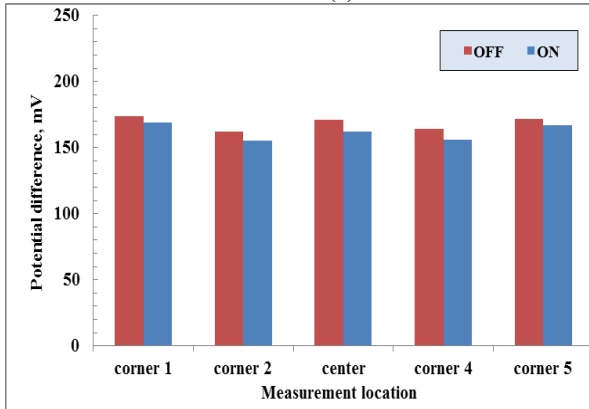


Figure 24: Polarization chart for configuration (ii) location (c)

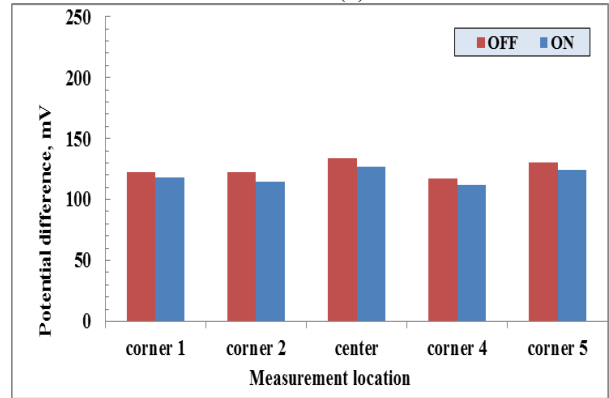


Figure 28: Polarization chart for configuration (iii) location (b)

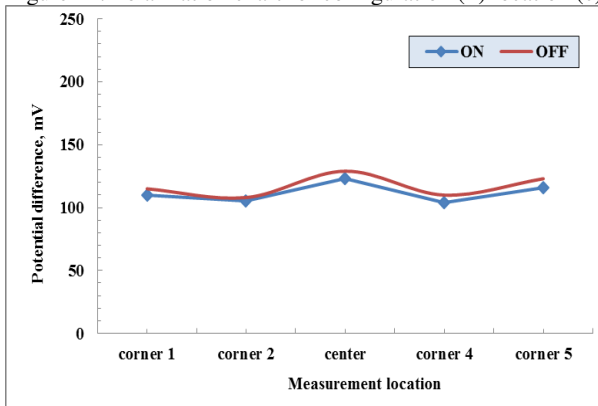


Figure 25: Average potential [ON& OFF] for configuration (iii) location (a)

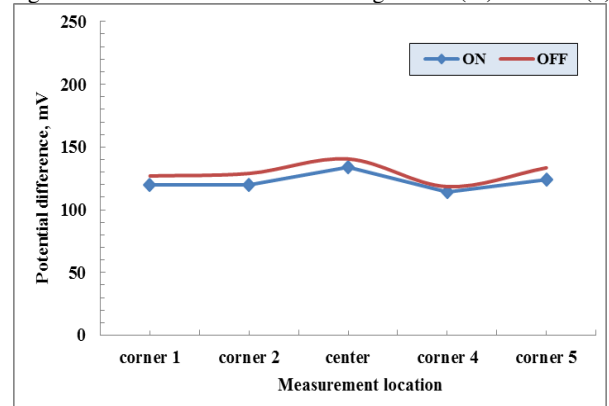


Figure 29: Average potential [ON& OFF] for configuration (iii) location (c)

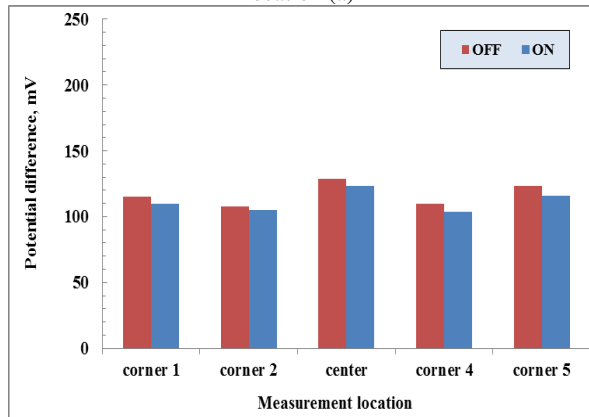


Figure 26: Polarization chart for configuration (iii) location (a)

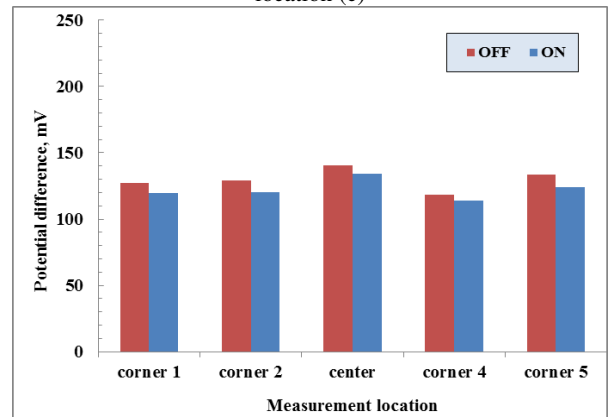


Figure 30: Polarization chart for configuration (iii) location (c)

## V. CONCLUSIONS

In view of experimental results obtained from present work, we conclude that:

- 1) Distributed anodes systems should be adopted to maintain adequate protection.
- 2) Distance between anodes should be determined with full consideration to “Proximity” effect phenomenon.
- 3) To avoid shading of some rebars by others it is preferable to locate anodes in the same plane of rebars or on both sides of this plane.

#### VI. NOMENCLATURE

DC	Direct Current
CP	Cathodic Protection
SRC	Steel Reinforced Concrete
SAS	Sacrificial Anode System
ICS	Impressed Current System
$\Delta E$	Average grid potential shift (Pon –Poff)
I	Average anodes current output for 3 days readings
Poff	Average $P_{off}$ for the five points measurements
Pon	Average $P_{on}$ for the five points measurements
RG	Apparent grid resistance ( $\Delta E/ I$ )

#### VII. ACKNOWLEDGEMENT

The authors are thankful to the Mechanical Power department students, faculty of engineering, Ain Shams University, year 2011-2012 for their contribution and assistance.

#### REFERENCES

- [1] Peabody A. W. “Control of Pipeline Corrosion” NACE, 2001.
- [2] Fontana M. G, and Greene N. D. “Corrosion engineering” McGraw-Hill, 1982.
- [3] David W. Whitmore and J. Christopher Ball “Galvanic Protection for Reinforced Concrete Structures” Concrete Repair Bulletin September/October 2005
- [4] Rengaswamy Srinivasan, Periya Gopalan, P. Ronald Zarriello, Christina J. Myles-Tochko, and James H. Meyer “Design of Cathodic Protection of Rebars in Concrete Structures: An Electrochemical Engineering Approach” Johns Hopkins Apl Technical Digest, Volume 17, Number 4 (1996)
- [5] Rob B. Polder “Cathodic Protection of Reinforced Concrete Structures in the Netherlands- experience and developments” HERON, VOL, 43, No.1 (1998) ISSN 0046-7316
- [6] Saad El-Deen E. M., Abd El-Ghany A. S., Desouky S. M “Simulating Cathodic Protection of Sheet Pile Walls Immersed in Saline Water” Journal of Environmental Science, Volume 11, No. 2 December, 2005, ISSN 1110-0826
- [7] NACE, Publication TCP, “Corrosion Control in Petroleum Production”, 1979.
- [8] Saad El-Deen E. M., Abd El-Ghany A. S., Desouky S. M “Comparison Between Single and Multi Anodes in Cathodic Protection Systems in Condensed Underground Piping Area”. Published in the Journal of Environmental Science, Vol. 23 Issue 1 2014, ISSN 1110-0826”
- [9] Saad El-Deen E. M., Abd El-Ghany A. S., Desouky S. M, Gomaa A. (2013) “Investigation of Performance of close Anode Cathodic Protection System Applied to a plane Metallic Grid”, Presented at the 16th international conference on petroleum, mineral resources and Development held in Cairo Egypt, Feb.,10-12
- [10] Saad El-Deen E. M., Abd El-Ghany A. S., Gomaa A. (2014) “EPRI Potential in Management of Corrosion Control for Steel Structures by Cathodic Protection Problems in Petroleum Industry”. Presented at the 17th International Conference on Petroleum, Mineral Resources and Development, held in Cairo Egypt, Feb., 09-11